# CHAPTER V
# SYNTHESIS AND CHARACTERIZATION OF NR/HMS-SO$_3$H COMPOSITES

In this Chapter, the sulfonic acid-functionalized mesoporous composites based on natural rubber (NR) and hexagonal mesoporous silica (HMS): (NR/HMS-SO$_3$H composite) was synthesized at difference MPTMS/TEOS ratios. All materials synthesized in this Chapter were prepared with the molar composition similarly to NR/HMS-8 as described in Chapter III. A series of NR/HMS-SO$_3$H composites was prepared via an *in situ* sol-gel process using tetrahydrofuran as the synthesis media. Tetraethylorthosilicate as the silica source, was simultaneously condensed with 3-mercaptopropyltrimethoxysilane in a solution of NR followed by oxidation with hydrogen peroxide to achieve the mesoporous composites containing propylsulfonic acid groups. The NR/HMS-SO$_3$H composites can take advantages from both surface functionalization with organo-sulfonic acid groups and hydrophobic polymer as natural rubbers to design the acidic composites with high mesoporosity and hydrophobicity. In addition, their structural, textural and physicochemical properties were investigated in comparison with those of pure silica HMS-T and acidic hexagonal mesoporous silica (HMS-SO$_3$H).

## 5.1 Thermogravimetric analysis (TGA)

The TG and DTA curves of HMS-SO$_3$H (0.1) and NR/HMS-SO$_3$H (0.1), as representative samples of HMS-SO$_3$H and NR/HMS-SO$_3$H materials, respectively, are shown in Figure 5.1. Both samples exhibited three-step weight loss. The endothermic change occurred up to 110 °C was due to loss of solvent and physisorbed water. The subsequent major weight loss consisting of two exothermic peaks observed between 250 and 450 °C, was attributed to the combustion of the propylsulfonic acid groups functionalized on the HMS structure [103]. The change of weight appearing at about 525 °C was related to condensation of surface silanol groups. Within this range, NR/HMS-SO$_3$H (0.1) gave higher weight loss (~17 wt.%) than HMS-SO$_3$H (0.1) (~12 wt.%). The result suggested the presence of NR in NR/HMS-SO$_3$H since the thermal decomposition of pure NR occurred at 368 °C [104]. Unfortunately, the range of thermal decomposition of NR was similar to propylsulfonic acid groups. Therefore, the exactl NR content of NR/HMS-SO$_3$H (0.1) could not be determined by TG/DTA technique. However, the NR content of NR/HMS-SO$_3$H materials should be closed to

that of NR/HMS (~10 wt.%) due to the similar NR loading used in the synthesis mixture.
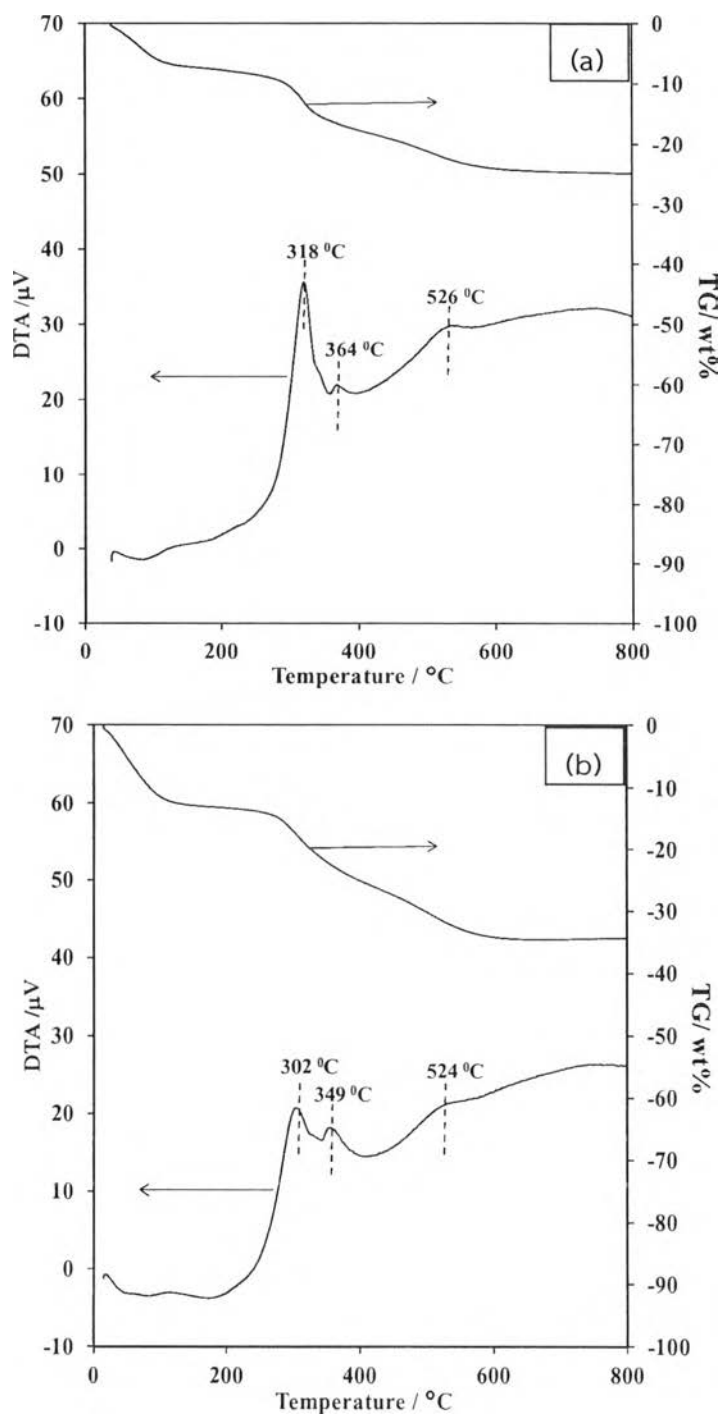


**Figure 5.1** Weight loss and DTA curves of (a) HMS-SO$_3$H (0.1) and NR/HMS-SO$_3$H (0.1) composite after removal of organic template by extraction.

The silica contents of HMS-SO$_3$H and NR/HMS-SO$_3$H prepared with different molar compositions as estimated by the TGA technique are summarized in Table 5.1. The amount of silica was decreased with increasing the MPTMS/TEOS ratio. HMS-SO$_3$H possessed the silica content in the range of 75.1–67.0 %, while a smaller amount of silica was observed for NR/HMS-SO$_3$H (65.6–58.1%). In addition, the elemental analysis by using CHN analyzer revealed that the removal of DDA by extracting with acidified ethanol was effective since the N content of HMS-SO$_3$H and NR/HMS-SO$_3$H were very low (<0.4%).

**Table 5.1** Silica content of HMS-T, HMS-SO$_3$H and NR/HMS-SO$_3$H composites synthesized under various conditions.

| Sample[a] | Silica content[b] (%) |
|---|---|
| HMS-T | *n.d.* |
| HMS-SO$_3$H (0.1) | 75.1 |
| HMS-SO$_3$H (0.2) | 67 |
| NR/HMS-8 | 78.5 |
| NR/HMS-SO$_3$H (0.1) | 65.6 |
| NR/HMS-SO$_3$H (0.2) | 61.7 |
| NR/HMS-SO$_3$H (0.4) | 58.1 |

*n.d.* = not determined.

[a] Number in parenthesis indicates the MPTMS/TEOS molar ratio.

[b] Determined by thermogravimetry technique.

## 5.2 XRD analysis

Figure 5.2 shows the XRD patterns of the pure silica HMS, HMS-SO$_3$H, NR/HMS-8 and NR/HMS-SO$_3$H composites after the extraction of template molecules. These materials exhibited one diffraction peak at 2-Theta in the range of 1.0-3.0 °, relating to characteristic (100) plane of hexagonal mesoporous structure. It can be seen that the introduction of organic species, either propylsulfonic acid group or NR, into HMS decreased the structural arrangement. The effect of the MPTMS/TEOS ratio on the hexagonal mesostructure was similar for both functionalized HMS and NR/HMS although the loss of structure ordering was more obvious for NR/HMS-SO$_3$H than for HMS-SO$_3$H.
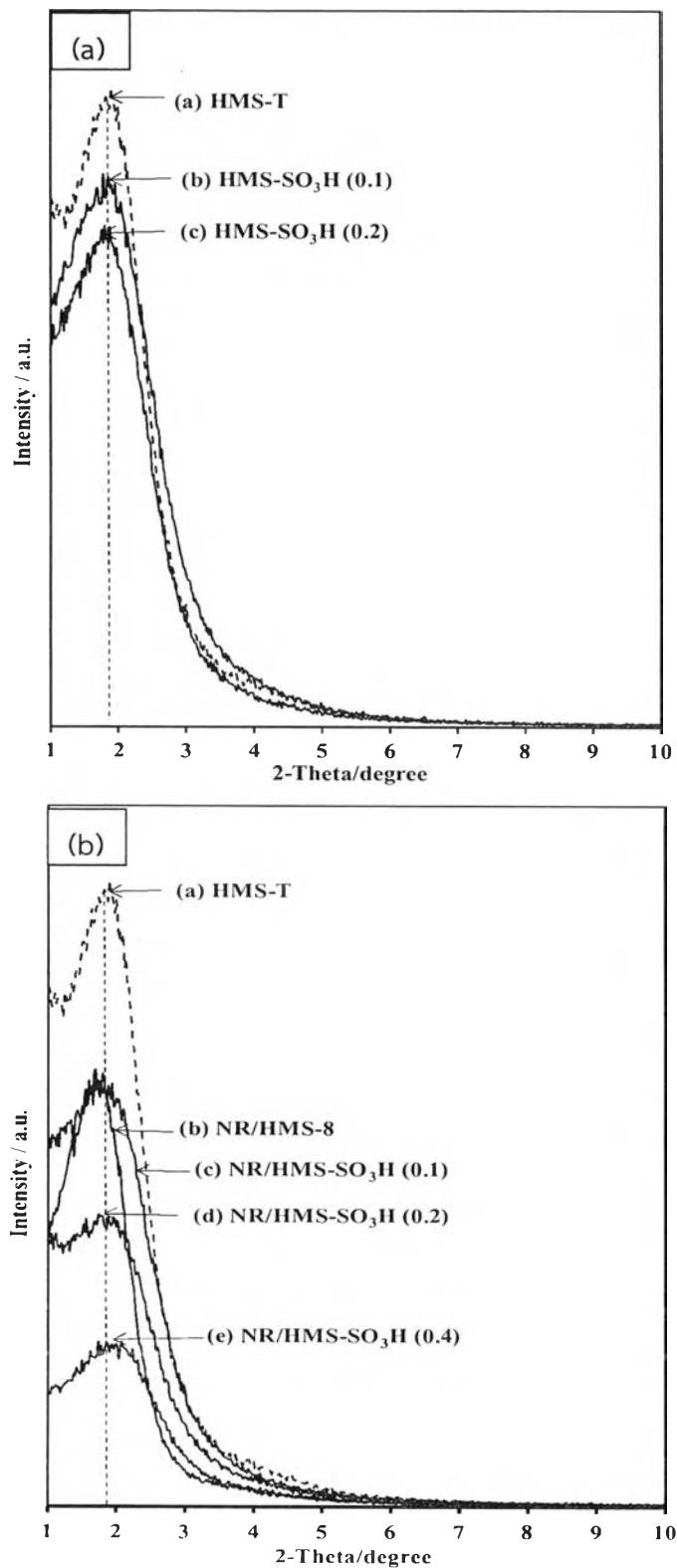
Figure 5.2 XRD patterns of (a) pure silica HMS-T, HMS-SO₃H and (b) NR/HMS-8, NR/HMS-SO₃H composites.

As shown in Table 5.2, an increase in the amount of MPTMS loading for the HMS-SO₃H series resulted in a systematic increase in $d_{100}$ and unit cell parameter, corresponding to thicken wall of silica framework. In addition, by comparing the structural data of NR/HMS-8 with that of pure silica HMS, the hexagonal unit cell and wall thickness were expanded with the presence of NR (Table 5.2). These results suggested that the NR molecules were incorporated in between the mesoporous channels, since the mesopore size is too small to accommodate the bulky NR molecules as mention in Chapter IV.

**Table 5.2** Structural properties of HMS-T, HMS-SO₃H and NR/HMS-SO₃H composites synthesized under various conditions.

| Sample[a] | $d_{100}$[b] (nm) | $a_0$[c] (nm) | $W_T$[d] (nm) |
|---|---|---|---|
| HMS-T | 4.3 | 5.0 | 1.8 |
| HMS-SO₃H (0.1) | 4.5 | 5.2 | 2.6 |
| HMS-SO₃H (0.2) | 4.7 | 5.4 | 2.8 |
| NR/HMS-8 | 4.9 | 5.7 | 2.5 |
| NR/HMS-SO₃H (0.1) | 4.4 | 4.8 | 2.7 |
| NR/HMS-SO₃H (0.2) | 4.5 | 5.2 | 2.8 |
| NR/HMS-SO₃H (0.4) | 4.4 | 5.1 | 3.0 |

n.d. = not determined.

[a] Number in parenthesis indicates the MPTMS/TEOS molar ratio.

[b] $d_{100}$ from XRD analysis.

[c] The repeat distance ($a_0$) between the pore centers of the hexagonal structure was calculated from $a_0 = 2d_{100}/3^{1/2}$.

[d] The framework wall thickness was determined by subtracting the BJH mesopore size from the repeat distance between pore centers.

Interestingly, the functionalization onto NR/HMS induced the unit cell contraction, while the thickness of pore wall was increased. This result suggested that the adding organofunctional groups to functionalize onto composite structure was affected the arrangement of the hexagonal mesostructure more obviously than pure HMS structure. Similarly to the case of HMS-SO₃H, the unit cell parameter and the wall thickness of NR/HMS-SO₃H were increased with the amount of MPTMS. It

can be rationalized from these results that the mesoporous structure of both HMS-SO$_3$H and NR/HMS-SO$_3$H was functionalized with the propylsulfonic acid group.

## 5.3 FTIR spectroscopy

The presence of NR or propylsulfonic acid groups in the HMS structure could be identified by using FTIR spectroscopy. As shown in Figure 5.3, the adsorption bands of the siliceous framework (Si–O–Si) of all mesoporous samples appeared between 1000 and 1300 cm$^{-1}$. The pure silica HMS exhibited a sharp band at 3740 cm$^{-1}$ and a broad band at around 3500 cm$^{-1}$, which can be respectively assigned to surface silanol groups as free and hydrogen-bonded species [23]. After the functionalization (HMS-SO$_3$H (0.1)), the bands related to the propylsulfonic acid groups were observed at 1360 cm$^{-1}$, corresponding to the S=O stretching of sulfonic acid groups, at 2850 and 2922 cm$^{-1}$ related to the C-H stretching of methylene groups, and around 3450 cm$^{-1}$, derived from the O-H stretching the sulfonic acid groups [105]. Simultaneously, the absorbance of free silanol band was largely decreased. These results indicated that the silica surface was modified by incorporating the organosulfonic groups.

On the other hand, NR/HMS-8 gave various characteristic bands of the NR structure at 3010, 2960, 2920, 2848, 1655, 1440 and 1390 cm$^{-1}$ [100, 101]. The band related to free silanol group (3740 cm$^{-1}$) was decreased, while the band of hydrogen-bonded silanol species (3500 cm$^{-1}$) was increased. The results suggested that the NR molecules were bound onto the HMS surface. By comparing the spectrum of NR/HMS-SO$_3$H (0.1) to that of NR/HMS, the bands representing –C=C– of the NR backbone at 3010, 2960, 1655 cm$^{-1}$ were decreased. It should be due to a high oxidizing power of H$_2$O$_2$ that can react with –C=C– of polyisoprene [106]. However, we did not observe any functional groups related to the possible oxidized products. The functionalization of propylsulfonic acid onto the surface of NR/HMS (NR/HMS-SO$_3$H) was confirmed by the band at 1360 cm$^{-1}$ and by a further decrease of free silanol group at 3740 cm$^{-1}$.
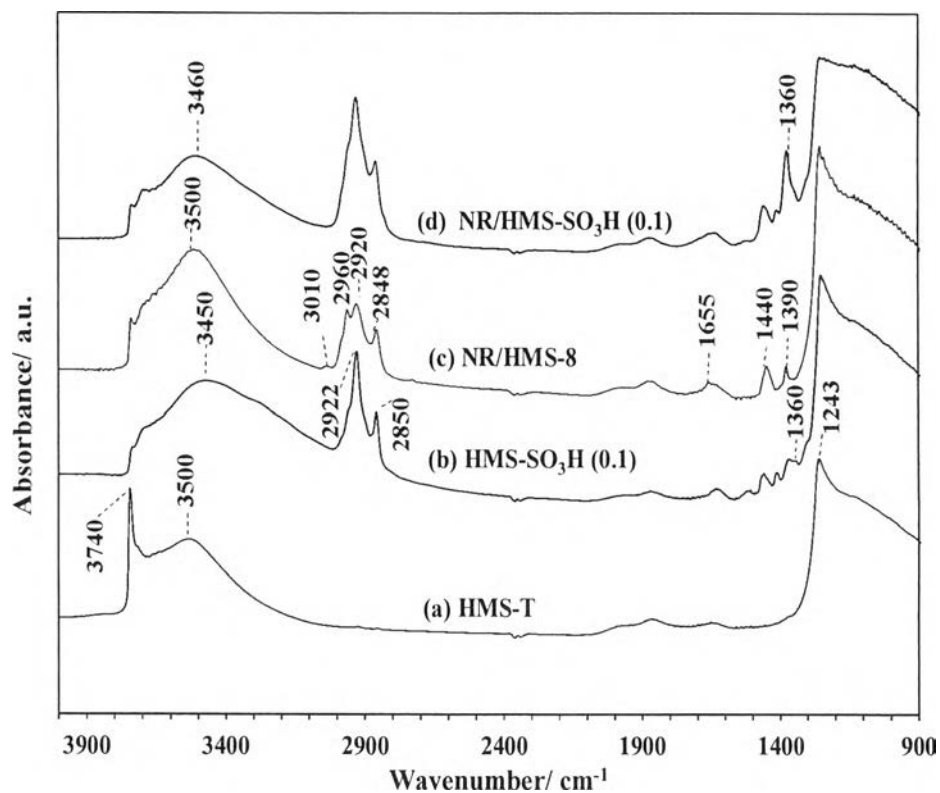
**Figure 5.3** FTIR spectra of the (a) pure silica HMS-T, (b) HMS-SO$_3$H (0.1), (c) NR/HMS-8 and (d) NR/HMS-SO$_3$H (0.1).

## 5.4 Solid state $^{29}$Si MAS NMR studies

Figure 5.4 shows $^{29}$Si MAS NMR spectra of pure silica HMS-T and NR/HMS-8 composites before and after the functionalization with propylsulfonic acid group. Three signals observed in sequence at -90, -101 and -109 ppm corresponded to Q$^2$ (Si(OSi)$_2$(OH)$_2$), Q$^3$ (Si(OSi)$_3$(OH)), and Q$^4$ (Si(OSi)$_4$) species, respectively, and other two signals found at -56 and -66 ppm were attributed to T$^2$ (RSi(OSi)$_2$(OH)) and T$^3$ (RSi(OSi)$_3$) sites, respectively, where R is referred to as the organo-functional group. It was clearly seen that the functionalization decreased the intensity of Q$^2$ and Q$^3$ concomitantly with the generation of T$^m$ species.
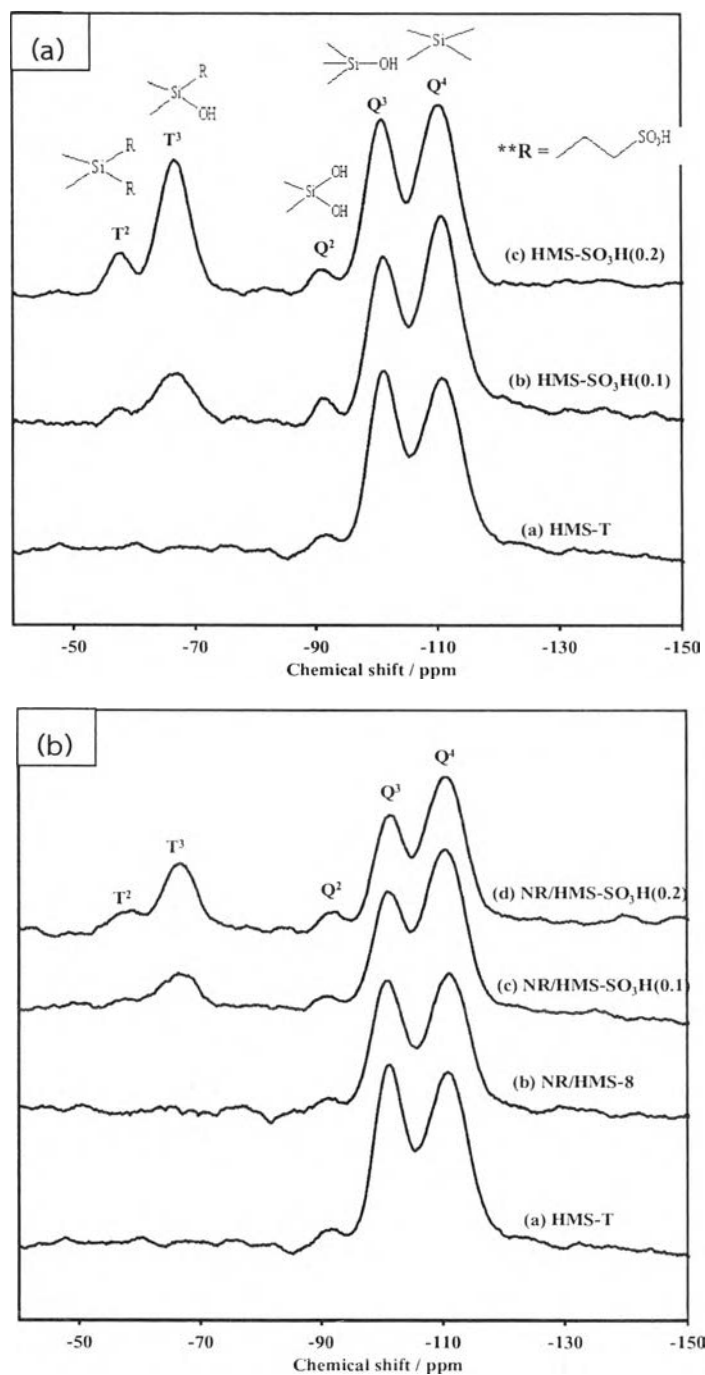
Figure 5.4 ^{29}Si MAS NMR spectra of (a) pure silica HMS-T and functionalized HMSs and (b) NR/HMS-8 composite and functionalized NR/HMS composites.

**Table 5.3** Relative intensities of the $T^m$ and $Q^n$ groups (obtained from the deconvolution of the $^{29}Si$ MAS NMR by using Origin Professional software (version 8.5)) and the sulfur contents (obtained from CHNS analysis) of HMS-T, HMS-SO$_3$H and NR/HMS-SO$_3$H composites synthesized under various conditions.

| Sample | $T^2$ (%) | $T^3$ (%) | $Q^2$ (%) | $Q^3$ (%) | $Q^4$ (%) | $(Q^2+Q^3)/Q^4$ (%) | $\Sigma T^m/\Sigma(T^m+Q^n)$ (%) | Sulfur content (mmol g$^{-1}$) |
|---|---|---|---|---|---|---|---|---|
| HMS-T | - | - | 3.4 | 40.5 | 56.1 | 78 | - | - |
| HMS-SO$_3$H (0.1) | 1.6 | 12.1 | 3.4 | 32.1 | 50.8 | N/A | 14 | 1.18 |
| HMS-SO$_3$H (0.2) | 5.3 | 23.9 | 2.2 | 28.1 | 40.4 | N/A | 29 | 1.55 |
| NR/HMS-8 | - | - | 2.6 | 39.1 | 58.3 | 72 | - | - |
| NR/HMS-SO$_3$H (0.1) | 1.7 | 11.7 | 2.5 | 31.1 | 53.0 | N/A | 13 | 0.94 |
| NR/HMS-SO$_3$H (0.2) | 5.4 | 20.6 | 2.0 | 25.4 | 46.7 | N/A | 26 | 1.59 |

*N/A* = not applicable.

More precisely, the $(Q^2+Q^3)/Q^4$ and $\Sigma T^m/\Sigma(T^m+Q^n)$ ratios determined from deconvolution of $^{29}Si$ MAS NMR spectra of these materials are summarized in Table 5.3. The primary NR/HMS-8 composite gave lower $(Q^2+Q^3)/Q^4$ ratio than the pure silica HMS-T, indicating smaller amount of free silanol group on the HMS surface with the presence of NR. This result was consistent with the FTIR results that suggested the covering of NR molecules on the mesoporous silica surface (Figure 5.3). With increasing the MPTMS/TEOS ratio used in the preparation of HMS-SO$_3$H and NR/HMS-SO$_3$H, the intensity of $T^m$ species as well as the $\Sigma T^m/\Sigma(T^m+Q^n)$ ratio were increased correspondingly with their sulfur content. Furthermore, the NR/HMS-SO$_3$H composites gave lower relative amount of $Q^2$ and $Q^3$ than the HMS-SO$_3$H synthesized with the similar MPTMS/TEOS ratio. It can be concluded that the NR/HMS-SO$_3$H composites had smaller content of free silanol group than the HMS-SO$_3$H materials.

## 5.5 Sulfur content and acidity measurement

The sulfur content and acidity of HMS and NR/HMS functionalized with propylsulfonic acid group as determined from CHNS elemental analysis and acid-base titration, respectively, are summarized in Table 5.4. Increasing the MPTMS/TEOS ratio of the synthesis mixture resulted in an increase in the sulfur content and

enhanced the acidity of the resulting materials. In all cases, the acidity value was less than the sulfur content, and the acidity/sulfur content ratio was continually decreased when the amount of MPTMS added was increased. These results suggested that the oxidation process by using $H_2O_2$ could not convert all of the thiol groups to the corresponding sulfonic acid. The conversion of sulfur to sulfonic acid for the HMS-$SO_3$H and NR/HMS-$SO_3$H series was in the range of 87−90 % and 72−88 %, respectively. The smaller extent of the sulfur conversion observed for the NR/HMS-$SO_3$H composites suggested that some mercaptopropyl groups were embedded in the NR layer, probably due to a hydrophobic attraction.

**Table 5.4** Sulfur contents (obtained from CHNS analysis) and acidity (obtained from acid-base titration) of HMS-$SO_3$H and NR/HMS-$SO_3$H composites synthesized under various conditions.

| Sample[a] | Sulfur content[b] mmol g$^{-1}$ | Acidity[c] mmol H$^+$ g$^{-1}$ |
|---|---|---|
| HMS-SO$_3$H (0.1) | 1.18 | 1.05 |
| HMS-SO$_3$H (0.2) | 1.55 | 1.35 |
| NR/HMS-SO$_3$H (0.1) | 0.94 | 0.83 |
| NR/HMS-SO$_3$H (0.2) | 1.59 | 1.18 |
| NR/HMS-SO$_3$H (0.4) | 2.22 | 1.61 |

*n.d.* = not determined.

[a] Number in parenthesis indicates the MPTMS/TEOS molar ratio.

[b] Determined by CHNS analyzer.

[c] Determined by acid-base titration with NaOH aq. (0.02M).

## 5.6 $N_2$ adsorption-desorption measurement

The $N_2$ adsorption-desorption isotherms and BJH pore size distribution of HMS-T and NR/HMS-8 with or without the functionalization are shown in Figures 5.5 and 5.6, respectively. The sorption isotherms of all materials exhibited the type IV shape isotherms in accordance with the IUPAC classification, with a hysteresis loop at $P/P_0$ ranging from 0.2-0.4, which are the characteristics of framework confined mesoporous materials. The large hysteresis loop observed at a high relative pressure

($P/P_0 > 0.8$) for these materials could be due to $N_2$ condensation inside the interparticle voids generated from their particle agglomerates.

As shown in Figure 5.5(a), the isotherms of HMS-SO$_3$H materials possessed lower $N_2$ adsorbed volume and smaller hysteresis loop at $P/P_0$ of 0.3-0.4 than that of HMS-T. Broader pore size distribution and smaller pore diameter were also observed for HMS-SO$_3$H when compared to the pure silica HMS-T (Figure 5.5(b)). The BET surface area ($S_{BET}$), pore diameter ($D_p$), total pore volume ($V_t$) and mesopore volume ($V_p$) were obviously decreased with increasing the amount of MPTMS loading (Table 5.5). These results supported that the organosilane was functionalized onto the primary HMS wall structure. The incorporation of organo-functional group in the HMS structure also reduced the hysteresis loop at $P/P_0 > 0.8$ (Figure 5.5.(a)) and decreased the external surface area ($S_{ext}$) (Table 5.5). Probably, the particle size of HMS-SO$_3$H materials was larger than the size of pure silica HMS-T particles.
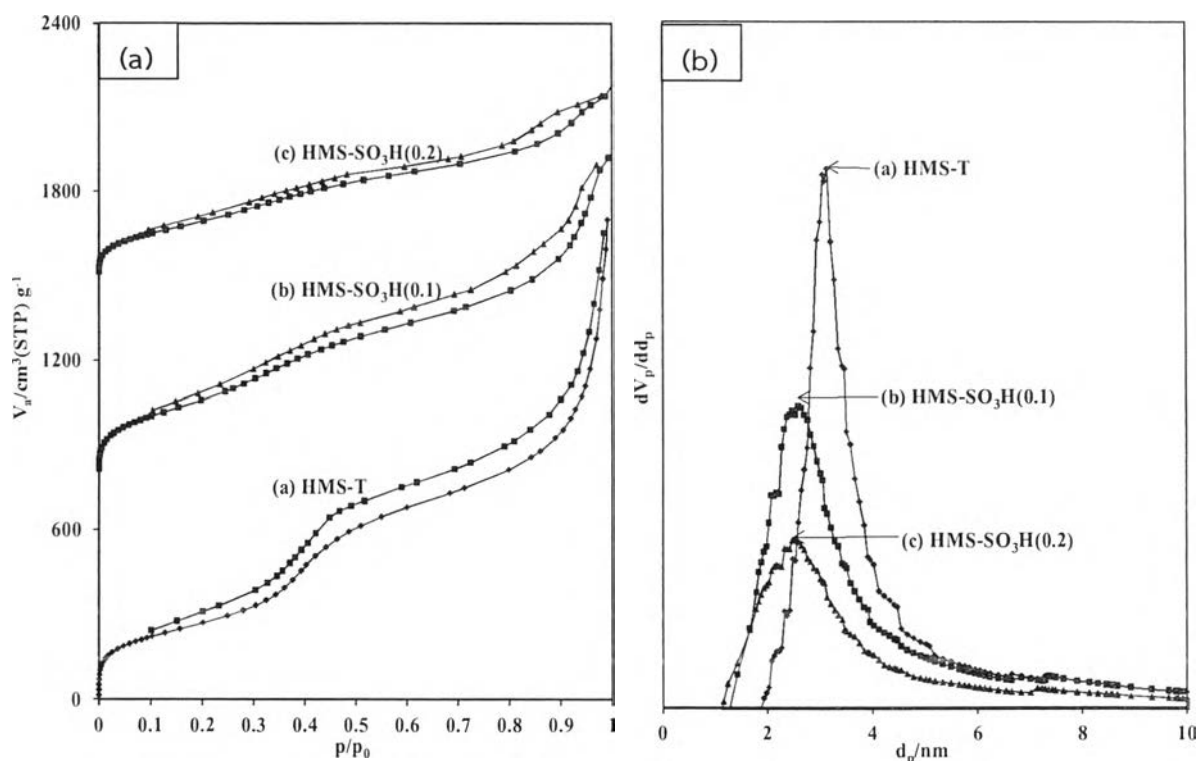


Figure 5.5 $N_2$ adsorption-desorption isotherms (a) and BJH pore size distribution (b) of the pure silica HMS-T and functionalized HMSs.

**Table 5.5** Textural properties of mesoporous and acidic mesoporous materials synthesized under various conditions.

| Sample[a] | $S_{BET}$[b] ($m^2 g^{-1}$) | $S_{ext}$[c] ($m^2 g^{-1}$) | $D_p$[d] (nm) | $Vt$[e] ($cm^3 g^{-1}$) | $V_p$[f] ($cm^3 g^{-1}$) |
|---|---|---|---|---|---|
| HMS-T | 852 | 548 | 3.15 | 2.57 | 0.73 |
| HMS-SO$_3$H (0.1) | 759 | 494 | 2.60 | 1.72 | 0.53 |
| HMS-SO$_3$H (0.2) | 673 | 274 | 2.54 | 1.00 | 0.43 |
| NR/HMS-8 | 570 | 268 | 3.19 | 1.96 | 0.42 |
| NR/HMS-SO$_3$H (0.1) | 560 | 399 | 2.33 | 2.28 | 0.35 |
| NR/HMS-SO$_3$H (0.2) | 543 | 288 | 2.33 | 1.80 | 0.34 |
| NR/HMS-SO$_3$H (0.4) | 524 | 151 | 2.08 | 1.18 | 0.29 |

*n.d.* = not determined.

[a] Number in parenthesis indicates the MPTMS/TEOS molar ratio.

[b] BET surface area.

[c] External surface area from *t*-plot curves.

[d] Pore diameter calculated using the BJH method.

[e] Total pore volume.

[f] Mesopore volume.

Comparing to the pure silica HMS-T, NR/HMS-8 showed smaller hysteresis loops at $P/P_0$ of 0.3-0.4 and of > 0.8 (Figure 5.6(a)). Although lower $S_{BET}$, $S_{ext}$, $V_t$ and $V_p$ were observed for NR/HMS-8, the pore size ($D_p$) was not significantly affected by the presence of NR (Table 5.5). This observation emphasized the location of NR molecules that favorably covered the external surface of mesoporous channels, resulting in the thicker pore wall.

The NR/HMS-SO$_3$H series revealed a continuous reduction of hysteresis loop at $P/P_0$ of 0.3-0.4 with increasing the MPTMS/TEOS ratio (Figure 5.6(a)). Similarly to the case of HMS-SO$_3$H, the pore size distribution became broader and the mesopore diameter was decreased (Figure 5.6(b)). However, their $S_{BET}$ and $V_p$ were decreased at much smaller extent than the HMS-SO$_3$H series when the MPTMS/TEOS ratio was

increased from 0.1 to 0.2 (Table 5.5). Probably, a part of the organo-functional groups were not bound onto the internal surface of primary mesopores. Some MPTMS molecules might condense with TEOS on the external surface at which the organic moieties stretched out to the NR layer covering the mesoporous channels due to the hydrophobic affinity of MPTMS and NR (Figure 5.7). The explanation was supported by a severe decrease in $S_{ext}$ when NR/HMS-SO$_3$H was prepared with the MPTMS/TEOS ratio of 0.4 (Table 5.5).
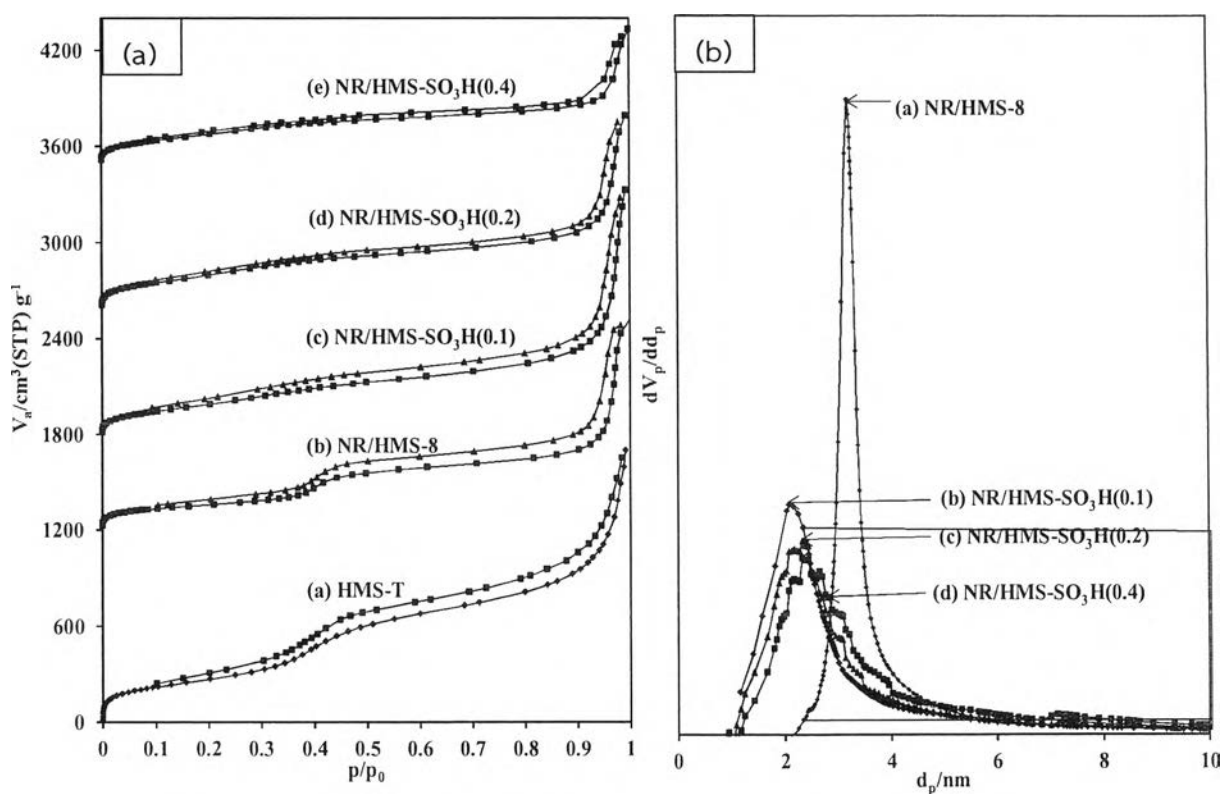
Figure 5.6 N$_2$ adsorption-desorption isotherms (a) and BJH pore size distribution (b) of pure silica HMS-T, NR/HMS and functionalized NR/HMS composites.
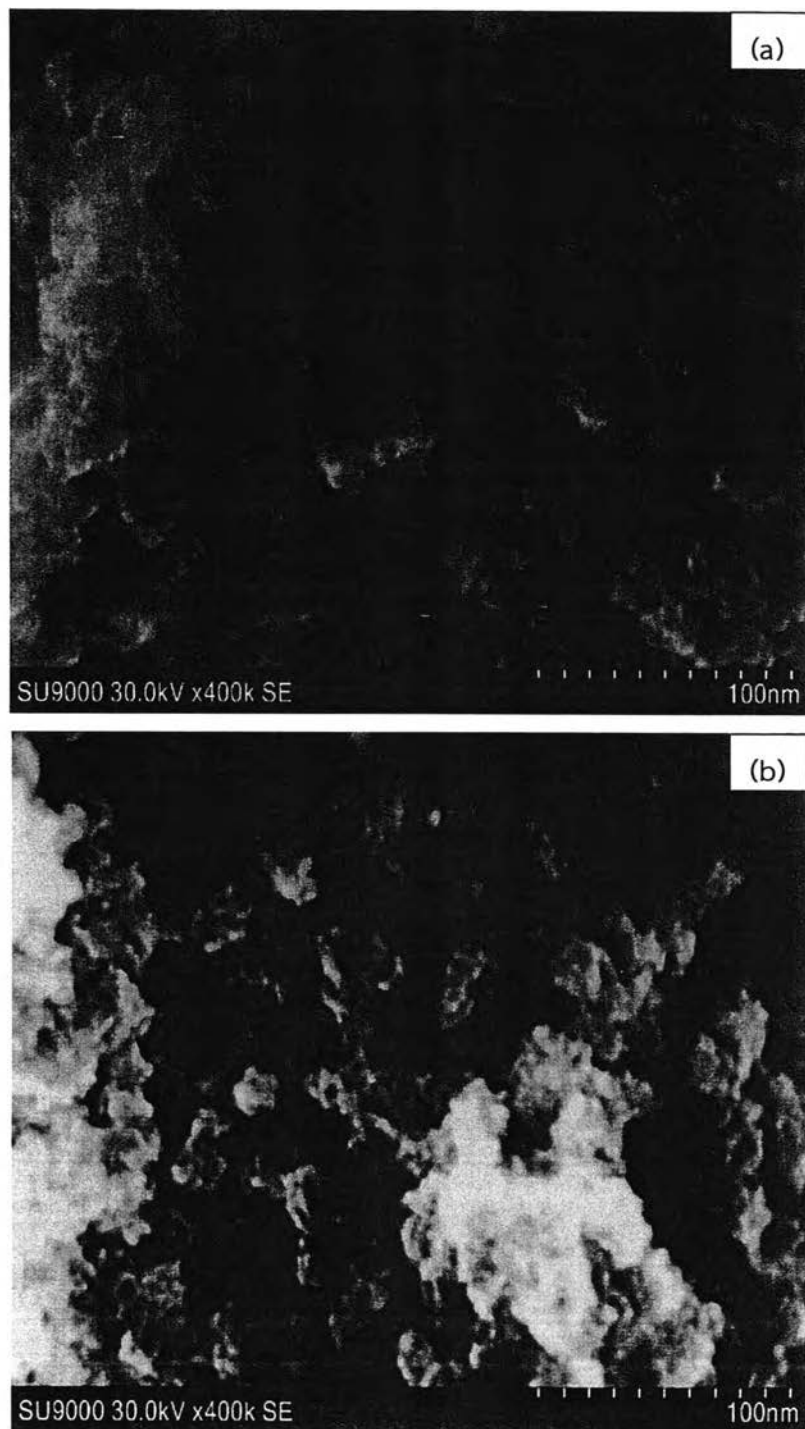
**Figure 5.7** Formation of the hexagonal array of silicate micellar rods and NR in the presence of MPTMS.

## 5.7 Electron microscopy

The morphology of the HMS-SO$_3$H (0.1) and NR/HMS-SO$_3$H (0.1) composites is depicted by the FE-SEM images in Figure 5.8. HMS-SO$_3$H (0.1) exhibited large aggregates of nanosized silica particles (Figure 5.8(a)). The low interparticle porosity was in agreement with the N$_2$ sorption isotherm of HMS-SO$_3$H (0.1) (Figure 5.5(a)) which revealed the small hysteresis loop at $P/P_0 > 0.8$. The presence of NR as the composite with the HMS structure (NR/HMS-SO$_3$H (0.1)) yielded smaller aggregates and better distribution of the particles ((Figure 5.8(b)). Moreover, it can be seen that the interparticle porosity was increased.

The STEM images of HMS-SO$_3$H (0.1) and NR/HMS-SO$_3$H (0.1) are shown in Figures 5.9(a) and (b), respectively. Both of the functionalized mesoporous materials possessed uniform framework-confined mesoporous channels of wormhole-like structure, similarly to the conventional HMS reported in Chapter IV.

SU9000 30.0kV x400k SE · · · · · · · · · · 100nm

SU9000 30.0kV x400k SE · · · · · · · · · · 100nm

**Figure 5.8** FE-SEM images at a magnification of x400,000 of (a) HMS-SO$_3$H (0.1) and (b) NR/HMS-SO$_3$H (0.1) composite.
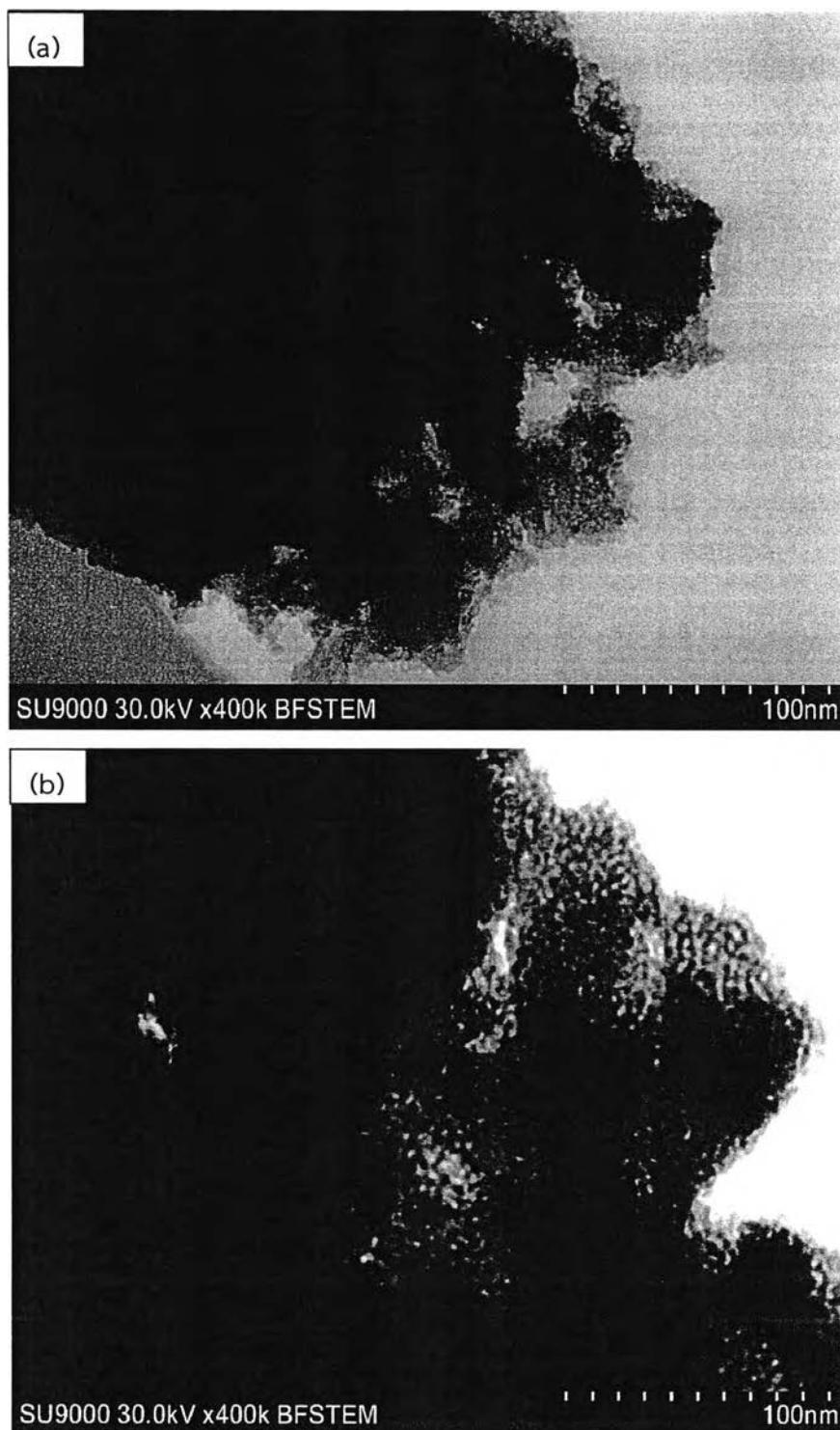
**Figure 5.9** STEM images at a magnification of x 400,000 of (a) HMS-SO$_3$H (0.1) and (b) NR/HMS-SO$_3$H (0.1) composite.

## 5.8 H$_2$O adsorption-desorption measurement

The technique of H$_2$O sorption measurement was used to evaluate the effects of propylsulfonic acid and/or NR on the hydrophobic properties of HMS-SO$_3$H and NR/HMS-SO$_3$H. As shown in Figure 5.10, the isotherm of pure silica HMS-T was classified as type IV. The large hysteresis loop and large volume of H$_2$O adsorbed were related to its high $S_{BET}$, $V_p$ and $D_p$ (Table 5.5). Taking into account its adsorption branch, it displayed a two-step uptake of H$_2$O, one at a medium and the other at a high relative pressure in which the former step was the adsorption of H$_2$O in the primary mesopores and the latter step was derived from H$_2$O filling into the interparticle voids. The H$_2$O molecules were not totally desorbed from the HMS-T surface as seen from the desorption branch end that remained unclosed, indicating a relatively strong bonding of H$_2$O on the silanol groups. Kimura et al. reported that some H$_2$O molecules were consumed for breaking the siloxane bridges (Si-O-Si) of the silicate framework [102].

The HMS-SO$_3$H series exhibited a similar shape of the isotherm to HMS-T (Figure 5.10(a)). The presence of the propylsulfonic acid in the mesoporous structure narrowed the hysteresis loop, indicating that H$_2$O desorbed from the functionalized surface more easily. Moreover, the decreased amount of silanol groups in HMS-SO$_3$H as evidenced by the $^{29}$Si MAS NMR data (Figure 5.4) reduced the monolayer adsorption volume of H$_2$O in the following order: HMS (82.3 cm$^3$ g$^{-1}$) > HMS-SO$_3$H (0.2) (70.3 cm$^3$ g$^{-1}$) $\approx$ HMS-SO$_3$H (0.1) (67.3 cm$^3$ g$^{-1}$).

The NR/HMS-8 and NR/HMS-SO$_3$H composites also exhibited the type IV shape isotherms of which the hysteresis loops were steeper than the pure silica HMS and the HMS-SO$_3$H series prepared with the similar MPTMS/TEOS ratio. The decrease in the H$_2$O affinity observed for the composites should be explained by the reduction of the exposed surface silanol groups as seen from the FTIR (Figure 5.3) and $^{29}$Si MAS NMR results (Table 5.3). Although the NR/HMS-SO$_3$H series possessed lower mesopore volume than the primary NR/HMS (Table 5.5), the monolayer adsorption volume of H$_2$O increased with the amount of sulfonic acid containing in the composites in following order: NR/HMS-8 (52 cm$^3$ g$^{-1}$) < NR/HMS-SO$_3$H (0.1) (58.7 cm$^3$ g$^{-1}$) < NR/HMS-SO$_3$H (0.2) (60.8 cm$^3$ g$^{-1}$) < NR/HMS-SO$_3$H (0.4) (80.3 cm$^3$ g$^{-1}$). It should be due to hydrophilicity of acidic function in the propylsulfonic acid group. These results indicated that the NR/HMS-SO$_3$H composites possessed higher hydrophobicity than HMS-SO$_3$H due to the incorporated NR molecules.
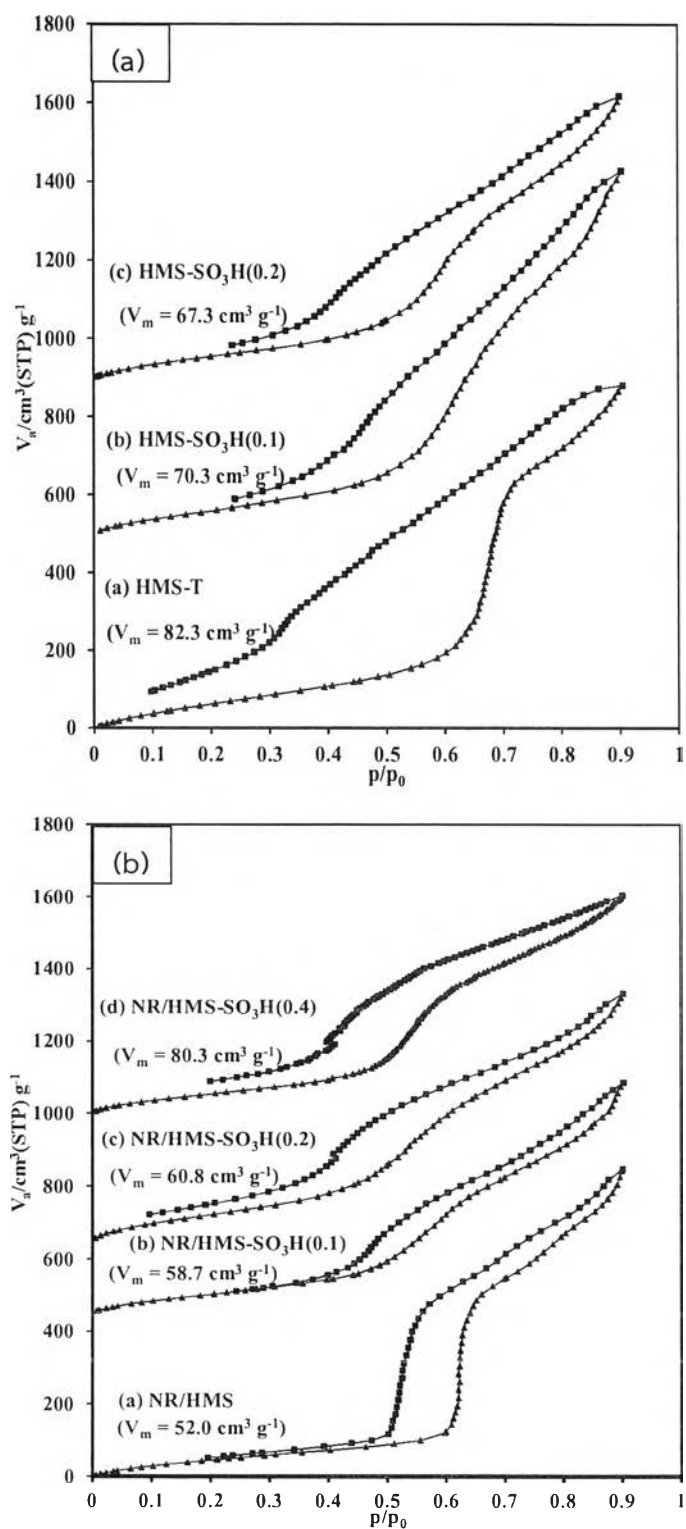
**Figure 5.10** $H_2O$ adsorption-desorption isotherms of (a) pure silica HMS-T and functionalized HMSs and (b) NR/HMS-8 and functionalized NR/HMS composites.

## 5.9 Pathway for the formation of NR/HMS-SO$_3$H composite.

According to the study in this Chapter, we would like to postulate the mechanism for the formation of NR/HMS-SO$_3$H via *in situ* sol-gel technique and simultaneous functionalization of mesostructure with organo-sulfonic acid groups as depicted in Figure 5.11. Firstly, TEOS and DDA were dissolved in the NR solution using THF as the synthesis media, subsequently H$_2$O, 3-mercaptopropyltrimethoxysilane (MPTMS) and H$_2$O$_2$ were added respectively. TEOS was hydrolyzed and simultaneously condensed together with MPTMS in the solution of natural rubber. The rearrangement of hexagonal mesostructure was occurred via the surfactant-templating as mention the mechanism in Chapter IV. However, the organo-functional group species could stretch out to the NR layer due to the hydrophobic affinity of MPTMS and NR. Therefore, some MPTMS molecules might condense with TEOS on the external surface. H$_2$O$_2$ was added in the synthesis mixture in order to oxidation thiol group of organosilane to sulfonic acid group. The acidic mesoporous composite take advantages of both HMS with high mesoporosity and NR as hydrophobicity improver. In the next Chapter, their catalytic activities were tested in the esterification of carboxylic acids with ethanol.
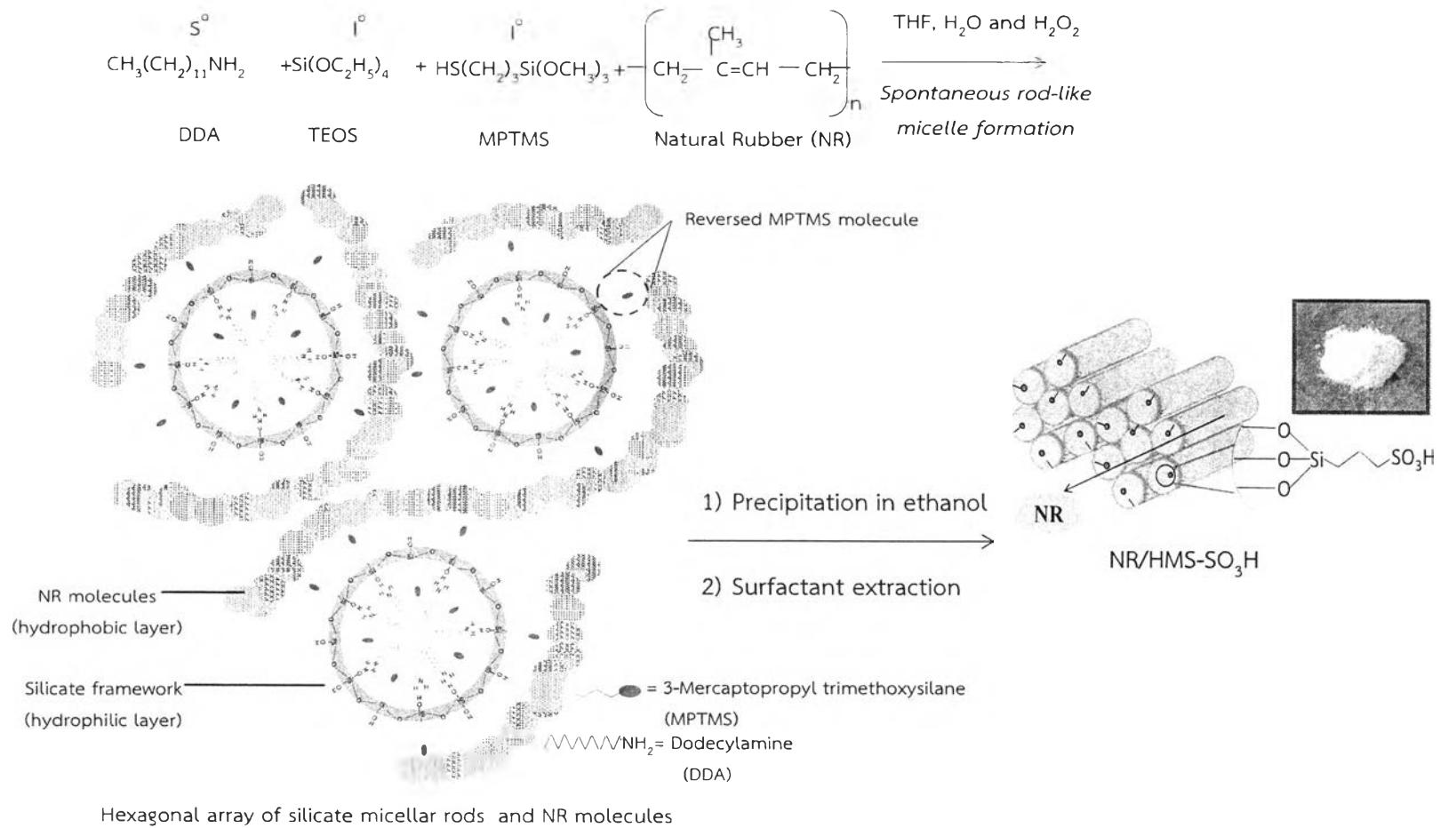
The reaction scheme shows:

$CH_3(CH_2)_{11}NH_2$ (S°) (DDA) $+ Si(OC_2H_5)_4$ (I°) (TEOS) $+ HS(CH_2)_3Si(OCH_3)_3$ (I°) (MPTMS) $+ \left[ CH_2 - \underset{CH_3}{\underset{|}{C}} = CH - CH_2 \right]_n$ Natural Rubber (NR)

THF, $H_2O$ and $H_2O_2$ → *Spontaneous rod-like micelle formation*

Reversed MPTMS molecule

NR molecules (hydrophobic layer)

Silicate framework (hydrophilic layer)

1) Precipitation in ethanol

2) Surfactant extraction

NR

NR/HMS-SO₃H

$-O-Si-(CH_2)-SO_3H$

= 3-Mercaptopropyl trimethoxysilane (MPTMS)

NH₂ = Dodecylamine (DDA)

Hexagonal array of silicate micellar rods and NR molecules

**Figure 5.11** Pathway for the formation of NR/HMS-SO₃H composite.